Hyperfine Interactions 123/124 (1999) 611–631

Noniron isotopes

O. Leupold [a,*], A.I. Chumakov [b], E.E. Alp [c], W. Sturhahn [c] and A.Q.R. Baron [d]

[a] *II. Institut für Experimentalphysik, Universität Hamburg, D-22761 Hamburg, Germany*
[b] *European Synchrotron Radiation Facility, BP 220, F-38043 Grenoble, France*
[c] *Advanced Photon Source, Argonne National Laboratory, Argonne, IL 60439, USA*
[d] *SPring-8, 323-3 Mihara, Mikazuki-cho, Sayo-gun, Hyogo 679-5198, Japan*

This article reports on experimental developments and first results for Mössbauer isotopes other than ^{57}Fe. We will restrict ourselves to basic features of the resonances of ^{169}Tm, ^{119}Sn, ^{83}Kr, ^{181}Ta, and ^{151}Eu and want to point out remarkable differences in instrumentation – like monochromator design – compared with ^{57}Fe. Some applications can be found in other sections of this issue.

1. Introduction

Like in conventional energy domain Mössbauer spectroscopy ^{57}Fe is the most widely used isotope in nuclear resonant scattering (NRS) of synchrotron radiation. A large variety of research on iron compounds is treated in the main part of this issue. This article is dedicated to other isotopes with energies between 6 and 25 keV, already used as nuclear scatterers in synchrotron radiation experiments, i.e., ^{169}Tm [1], ^{119}Sn [2,3], ^{83}Kr [4,5], ^{181}Ta [6], and ^{151}Eu [7,8]. Some relevant nuclear properties of these isotopes are summarized in table 1. Other isotopes which are of special interest for NRS of synchrotron radiation or which have been observed by NRS but are not treated in this article, like ^{161}Dy [8], are also listed in this table.

These isotopes are interesting from different points of view. They may offer access to physical phenomena besides those that can be studied by spectroscopy on the transition metal iron. Examples are pure spin magnetism and valence fluctuations in the rare earth compounds (^{151}Eu). Besides that, it is a challenge for the experimentator to develop new X-ray optics and to improve beamline components for energies different from 14.4 keV.

2. ^{151}Eu

One very interesting nucleus is ^{151}Eu with a resonance energy of 21.5417 keV. The numerous spectroscopic applications of this resonance benefit from the two valence states of europium. The Eu^{2+} ion with the magnetic $4f^7$ ($^8S_{7/2}$) state is an ex-

* Present address: European Synchrotron Radiation Facility, BP 220, F-38043 Grenoble, France.

Table 1
Several Mössbauer transitions in the energy range 6–30 keV and lifetimes longer than 1 ns.[1] Displayed are the following quantities: isotope – Mössbauer isotope, energy – Mössbauer transition energy, $t_{1/2}$ – half life of the Mössbauer level, Γ_0 – energy width of the Mössbauer level, α – internal conversion coefficient, abund. – natural abundance of the Mössbauer isotope, σ_0 – nuclear resonance cross-section.

Isotope	Energy (keV)	$t_{1/2}$ (ns)	Γ_0 (neV)	α	Abund. (%)	σ_0 (10^{-20} cm^2)
^{40}K	29.56(7)	4.25(6)	107.3	6.6(5)	0.012	28.7
^{57}Fe	14.4130(1)	97.81(14)	4.665	8.21(12)	2.14	255.7
^{73}Ge	13.263(15)	2953(23)	0.154	1095(55)	7.76	0.76
^{83}Kr	9.405(1)	147(4)	3.10	19.6(7)	11.55	107.5
^{119}Sn	23.879	17.75(12)	25.7	5.12(10)	8.58	140.3
^{149}Sm	22.494(11)	7.12(11)	64.07	50(10)	13.83	7.1
^{151}Eu	21.5417(5)	9.7(3)	47.03	28.60(15)	47.82	23.8
^{161}Dy	25.655(3)	28.2(9)	16.18	2.9(3)	18.88	95.3
^{169}Tm	8.41031(2)	4.00(10)	114.05	268(5)	100.00	25.8
^{181}Ta	6.2155(2)	6050(120)	0.075	70.5(3)	99.99	110

cellent example of pure spin magnetism, therefore, magnetic properties can be easily monitored with the ^{151}Eu resonance. Together with the Eu^{3+} ion with its nonmagnetic $4f^6$ ($^7F_0$) configuration of the 4f shell, europium compounds offer the possibility to study, e.g., temperature- and pressure-dependent valence transitions and the phenomenon of valence fluctuations. For Mössbauer experiments utilizing this isotope, see [9].

The resonance was first observed in nuclear forward scattering (NFS) at the ESRF in 1995 [7] and in nuclear inelastic scattering (NIS) at TRISTAN (KEK, Tsukuba) [8]. Despite this rather recent development several NFS experiments have already been performed. Some are described in this section, further applications in high pressure research [11] and on valence fluctuations [12] are presented elsewhere in this issue.

The nuclear properties (cf. figure 1, table 1) are challenging by themselves. The short lifetime $\tau = 14.1$ ns promises a strong delayed intensity due to the larger nuclear bandwidth compared with ^{57}Fe. On the other hand, the use of very thick absorbers ($t_{\mathrm{eff}} \gg 10$) should be avoided, since the speed-up shifts the resonantly re-emitted intensity close to time zero, where detectors and electronics are usually blocked due to the strong prompt pulse, which has to be suppressed by electronic means. In the experiment a reasonable compromise has to be found.

This section deals with the basic features of NFS at the ^{151}Eu resonance including instrumentational aspects. The high resolution monochromator for 21.54 keV will be treated in some detail, an extensive treatment of X-ray optics in general is given elsewhere in this issue [13].

[1] In Mössbauer Effect Data Center, Asheville, NC 28804-3299, USA. In the case of Kr, Eu, Sn and Ta we have used updated numbers which were recently determined at synchrotron radiation sources.

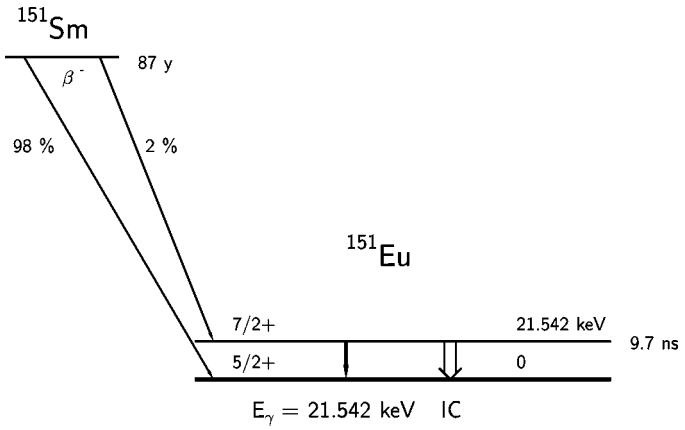

Figure 1. Partial nuclear decay scheme of ^{151}Eu from its parent nucleus ^{151}Sm. The (theoretical) total conversion coefficient is $\alpha = 28.6$ [9], the mean lifetime $\tau = 14.1$ ns of the ^{151}Eu excited nuclear level corresponds to a natural linewidth $\Gamma_0 = 48$ neV $\Leftrightarrow$ 0.67 mm/s.

2.1. Nuclear properties and hyperfine interaction

The $7/2 \rightarrow 5/2$ M1-transition of ^{151}Eu at 21.54 keV is mainly used in Mössbauer spectroscopy of europium compounds. The partial decay scheme for ^{151}Eu including the decay from the almost exclusively used mother isotope ^{151}Sm is shown in figure 1. Due to the high natural abundance of ^{151}Eu , 47.8%, it is not necessary to use isotopically enriched material.

The long lifetime of the ^{151}Sm parent nucleus makes the standard SmF_3 radioactive sources very convenient for Mössbauer spectroscopy. On the other hand, the short lifetime of the 21.54 keV Mössbauer level causes a rather large natural linewidth, which – together with the high spins of the nuclear states – makes a determination of quadrupole interactions very difficult in standard Mössbauer spectroscopy. Moreover, SmF_3 sources usually exhibit a large line broadening, up to $\approx$2 mm/s, which are most probably due to unresolved quadrupole interactions. Therefore, NFS of synchrotron radiation promises a more precise determination of quadrupole interactions.

The resonance energy of ^{151}Eu was determined as 21541.7 ± 0.5 eV with NFS [7] and as 21541.49 ± 0.16 eV with NIS [8]. Both values are in excellent agreement in contrast to the widespread range of other energy values given in the literature[2] [9,10].

The energy calibration was performed according to Bond [14], adopting the Si(12 12 8), Si(12 $\overline{12}$ 8) and Si(13 13 3), Si(13 $\overline{13}$ 3) reflections on a silicon single crystal in almost backscattering geometry [7] or using a combination of high indexed Bragg/Laue reflections [8].

The effect of hyperfine interactions on the ^{151}Eu nuclei is depicted in figure 2. By a proper choice of the direction of an external magnetic field one can select either $\Delta m = \pm 1$ or $\Delta m = 0$ transitions, when studying ferromagnetic compounds, and

[2] In [10] one can find two values differing by 8 eV!

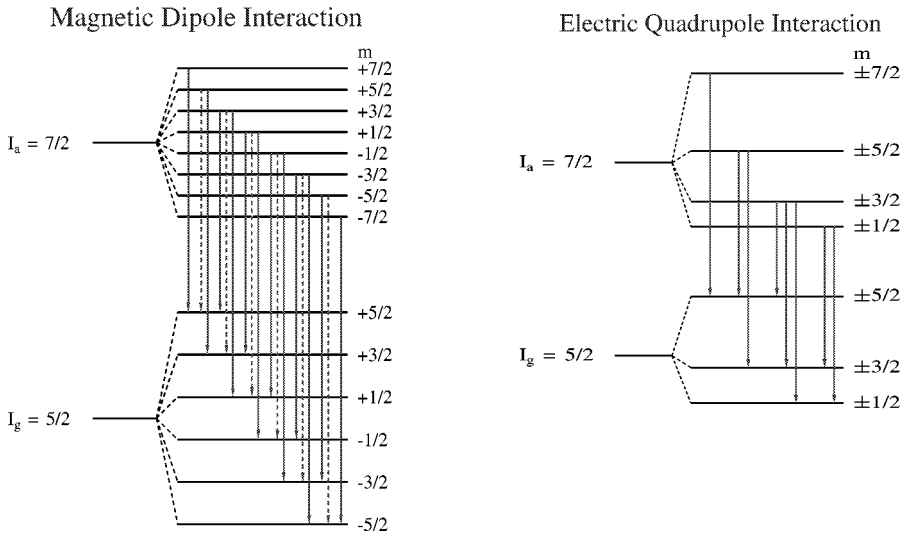

Figure 2. Hyperfine interactions acting on the ^{151}Eu nuclear levels. Left: magnetic hyperfine interaction, which yields 18 resonance lines in the general case; the full lines represent $\Delta m = \pm 1$ transitions, the dashed lines $\Delta m = 0$ transitions; the latter are not excited when an external field is aligned parallel to the beam direction. Right: electric quadrupole interaction, here shown for an asymmetry parameter $\eta = 0$, which yields 8 resonance lines.

simplify the time spectra remarkably (see below). On the other hand, one may easily see that the quadrupolar split lines cover only a range of about 0.8 mm/s, when the quadrupole interaction parameter takes a value of $eQ_{\mathrm{g}}V_{zz}/2 = 2$ mm/s, where Q_{g} is the quadrupole moment of the nuclear ground state. However, due to the high nuclear spins $I_{\mathrm{g}} = 5/2$ and $I_{\mathrm{e}} = 7/2$ for the ground and excited state, respectively, a determination of the asymmetry parameter η is in principle possible, also with polycrystalline samples and without external magnetic fields.

2.2. Experimental

All experiments described in this section were performed at the Nuclear Resonance Beamline (BL11, I D18) [15] at the European Synchrotron Radiation Facility (ESRF). The storage ring was operated either in the 32-bunch mode, giving a bunch distance of 88 ns, or in the 16-bunch mode corresponding to a bunch distance of 176 ns. The experimental set-up is shown in figure 3.

The monochromatization of the synchrotron radiation beam is performed in two steps. A cooled double crystal Si(1 1 1) high heat load monochromator with fixed exit delivers an energy bandwidth of about 6 eV. The subsequent high resolution monochromator was designed in nested configuration according to the suggestion in [16]. It consists of an outer Si(8 0 0) channel-cut crystal ($\theta_{\mathrm{B}} = 25.08°$), cut with an asymmetry parameter $b = -1/14$ in order to increase the angular acceptance, and an inner symmetric Si(12 4 4) channel-cut crystal ($\theta_{\mathrm{B}} = 44.66°$) which has a theoretical angular

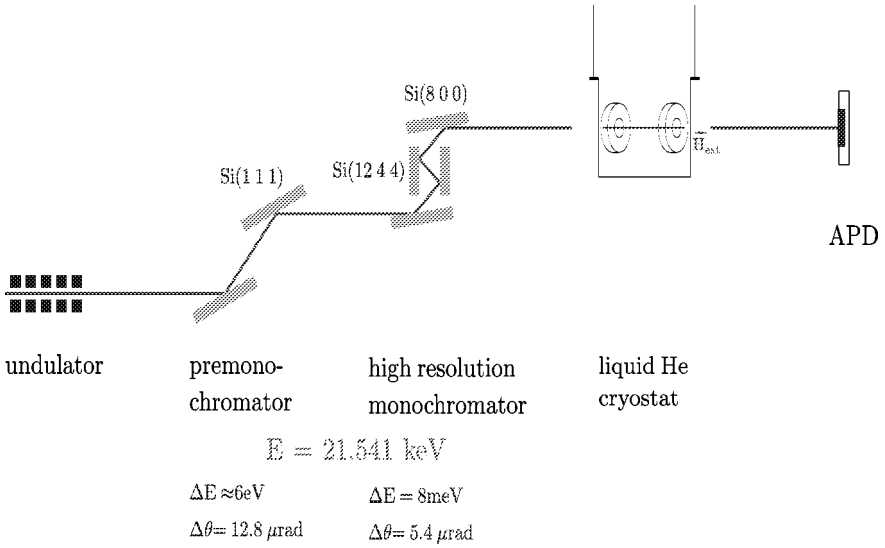

Figure 3. Typical experimental set-up for ^{151}Eu NFS experiments at the nuclear resonance beamline ID18 at ESRF [15].

width of 0.36 μrad. This corresponds to an energy bandwidth of 7.8 meV. Due to the Bragg angle of the Si(12 4 4) channel-cut crystal close to 45° the degree of polarization of the delivered beam is almost 100% linear in the electron orbit. The radiation was detected by a silicon-based fast avalanche photodiode (APD) [17] with a time resolution of about 1 ns. For a review on fast detectors, cf. [18]. The strong signal of the prompt electronic scattering was electronically blocked up to ≈8 ns. Accordingly, the time window for detection of the decay of the nuclear exciton could be opened only from ≈8 ns on.

In the first NFS experiment [7] a mixture of divalent EuS and trivalent Eu_2O_3 powders[3] was taken as a sample. The ratio of ^{151}Eu content of the two components was adjusted to 1 : 5 ($EuS : Eu_2O_3$), which, according to calculations made in advance, gives the highest delayed resonant counting rate in the experimental time window.

Standard Mössbauer experiments at room temperature have shown that the hyperfine parameters of the two modifications of Eu_2O_3, cubic and monoclinic, are the same within the experimental error. The isomeric shift with respect to EuF_3 is $+1.03$ mm/s and the quadrupole interaction parameter $eQ_gV_{zz}/2$ is -2.6 mm/s. EuS shows no quadrupole interaction. Its isomeric shift at room temperature is -11.6 mm/s [9]. This combination of Eu_2O_3 and EuS was chosen to facilitate the observation of quantum beats produced by the large isomer shift between Eu^{2+} and Eu^{3+}.

The nuclear resonance was identified by measuring the rocking curve of the high resolution Si(12 4 4) channel-cut crystal recording the delayed quanta. The rocking

[3] Eu_2O_3 was enriched to 97% in ^{151}Eu, EuS had the natural isotope abundance.

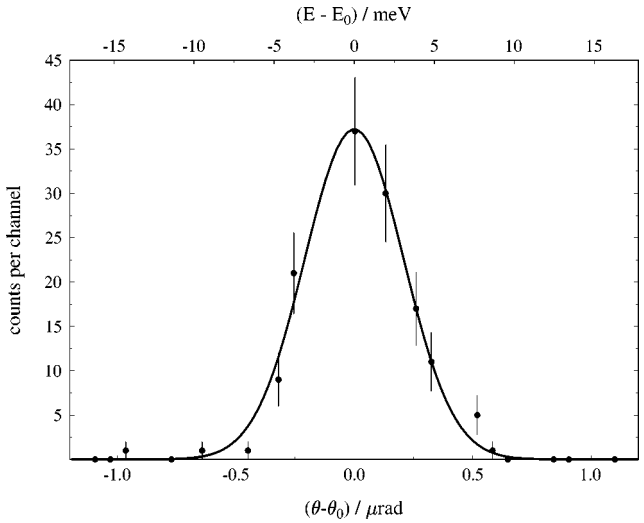

Figure 4. Rocking curve of the "inner" Si(12 4 4) channel-cut crystal of the high resolution monochromator recorded by detecting the delayed nuclear scattered photons only (i.e., photons in a time window from 8 to 60 ns) [7].

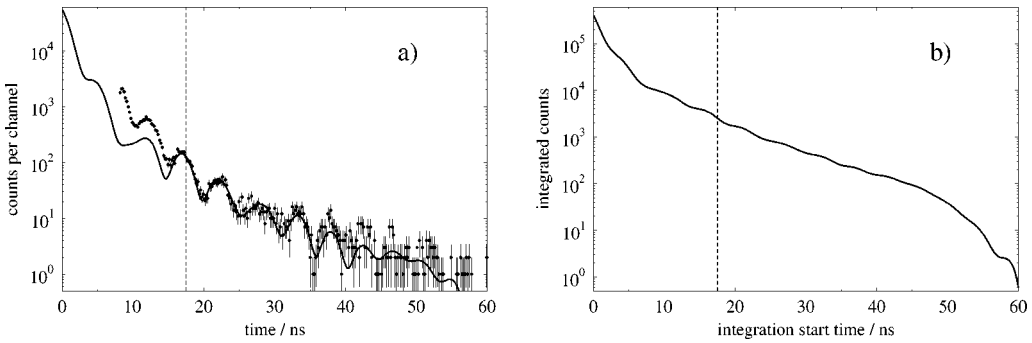

Figure 5. (a) Time spectrum of the Eu_2O_3/EuS powder mixture. The spectrum was recorded for 26 min in 32-bunch mode with an average resonant counting rate of $\approx$20 s^{-1}. (b) Integration of the theoretical simulation from (a). Only 0.7% (2.7%) of the delayed intensity is observed in the undisturbed time window after 17 ns (8 ns). Note the logarithmic intensity scale!

curve shown in figure 4 was obtained with a measuring time of only 1 s per point. The solid line is a fit with a Gaussian curve. It yields an experimental energy bandwidth of 7.3 meV for the high resolution monochromator.

Figure 5(a) shows the time spectrum of the Eu_2O_3/EuS powder mixture. Data evaluation was performed from 17 ns on (vertical dashed line), since the time response of the detector system was not linear in the range from 8 to 17 ns. The simulation yields 11.8(1) mm/s for the difference of the isomer shifts and a quadrupole interaction parameter for Eu_2O_3 of $-2.43(5)$ mm/s. All fits and simulations shown in this section were done with the program package CONUSS [19].

In figure 5(b) we display the time integrated delayed intensity as determined by the simulation, extended to $t = 0$, i.e., the time instant of excitation by the ≈100 ps long synchrotron radiation pulse. One can easily see the importance of setting the time window as close as possible to $t = 0$, in order to detect as much delayed intensity as possible. One possibility to get closer to $t = 0$ is the application of a crossed polarizer/analyzer set-up as earlier done for the ^{57}Fe resonance [20]. In fact, this was the reason for choosing the (12 4 4) reflection for the inner crystal and sacrifice a (possible) better energy resolution and larger angular acceptance when using a higher indexed inner channel-cut crystal. Unfortunately, the crossed polarizer/analyzer experiment has not yet been successful.

2.3. Examples

After this first basic experiment several applications at the ^{151}Eu resonance were performed at the ID18 beam line. As mentioned above, the large difference in isomer shift between the Eu^{2+} and the Eu^{3+} valence states makes NFS on europium compounds an almost ideal tool to determine the valence of the Eu atom/ion, by using reference samples of well-known isomer shift upstream or downstream of the sample under study. This technique was successfully applied at the ^{57}Fe resonance [21,22]. It is worthwile to note that – in contrast to conventional Mössbauer spectroscopy – a direct determination of the isomer shift is not possible in a single NFS measurement without reference sample, due to the broadband excitation by the synchrotron radiation pulse. In the case of ^{151}Eu there exist two standard compounds, the divalent EuS and the trivalent EuF_3. For demonstration of the effect of the isomer shift relative to a reference sample, we measured a powder sample of EuS and EuF_3 both alone and sandwiched together. The results are shown in figure 6.

- Figure 6(a): The time spectrum of a EuS powder sample can be fitted with a single resonance line, assuming a slight thickness inhomogeneity, which smears out the expected Bessel minimum.
- Figure 6(c): Time spectrum of a EuF_3 powder sample. This spectrum cannot be fitted with a single line only. The Bessel minimum is pronounced and excludes the possibility of a large thickness distribution. The best fit result was obtained when assuming a quadrupole interaction $eQ_gV_{zz}/2 = 1.7 \pm 0.25$ mm/s together with an asymmetry parameter of the EFG $\eta = 0.8$. The sign of V_{zz} cannot be determined, again due to the broad bandwidth of the exciting beam compared with the nuclear level width.
  Another successful approach to fit the EuF_3 time spectrum was found by Pleines [23]. She fitted the EuF_3 time spectrum with two resonance lines with relative intensity about 4 : 3 and energy difference ≈0.7 mm/s. This is in fact a very good approximation of the quadrupole spectrum with large η found by us.
  The unavoidable line broadening of a standard SmF_3 Mössbauer source obscured this splitting of the EuF_3 resonance in conventional Mössbauer spectra [23].

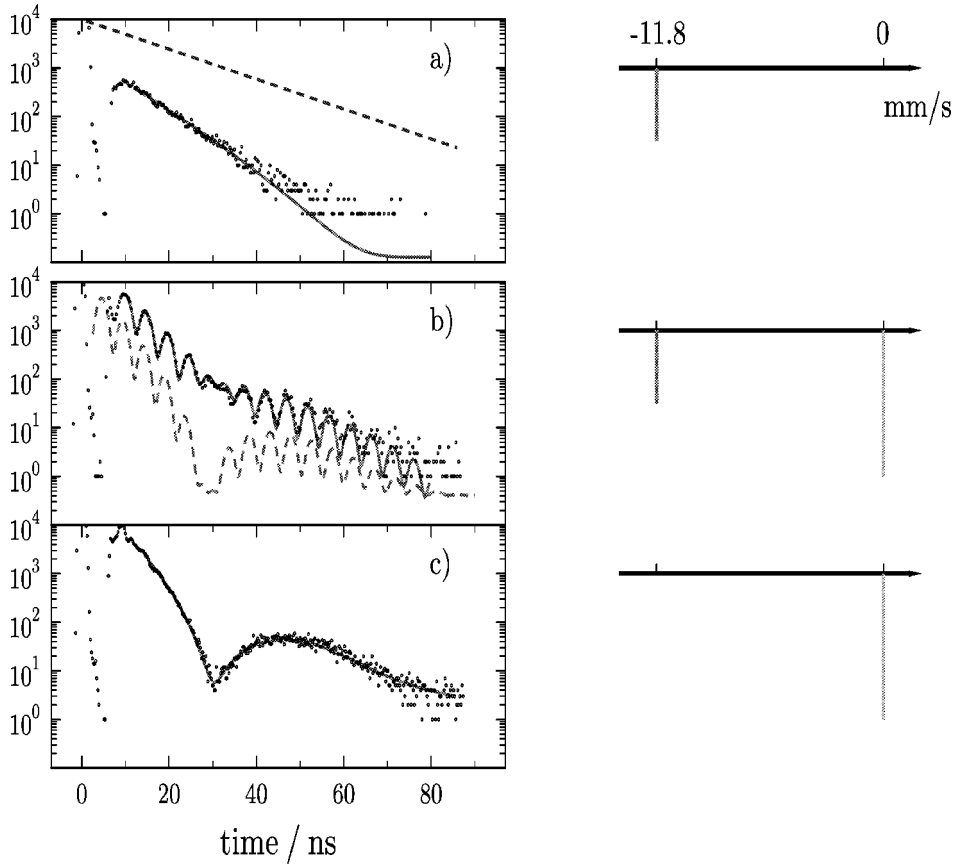

Figure 6. (a) Time spectrum of a EuS powder sample. The dashed line corresponds to a decay with the natural lifetime. (b) Time spectrum of a EuS/EuF_3 powder sample "sandwich". The dashed line resembles the shape of the spectrum of an "ideal sandwich" with two samples of identical thickness. (c) Time spectrum of a EuF_3 powder sample. The stick diagrams on the right visualize the position of the resonance lines in energy scale. The (small) line broadening of the EuF_3 resonance due to quadrupole splitting is neglected in the stick diagram.

- Figure 6(b): The time spectrum of the EuS/EuF_3 sandwich clearly reveals the large isomer shift between the Eu^{2+} and the Eu^{3+} states, exhibiting fast quantum beats with a period of $\approx$5 ns. The fitted difference in isomer shift $\delta(\mathrm{IS}) = 11.8 \pm 0.05$ mm/s corresponds to an energy of $8.5 \cdot 10^{-7}$ eV $\Leftrightarrow$ 205 MHz. With the use of the EuS isomer shift reference the determination of the sign of the quadrupole interaction parameter for EuF_3 is possible, in principle. However, at large η the spectrum of EuF_3 is almost symmetric, which makes an unambiguous determination difficult. However, the χ^2 of the fits favours the negative sign.
  The intensity at the Bessel minimum around 30 ns does not reach the zero level, due to the different thicknesses of the two samples, but only reduces the quantum beat contrast.

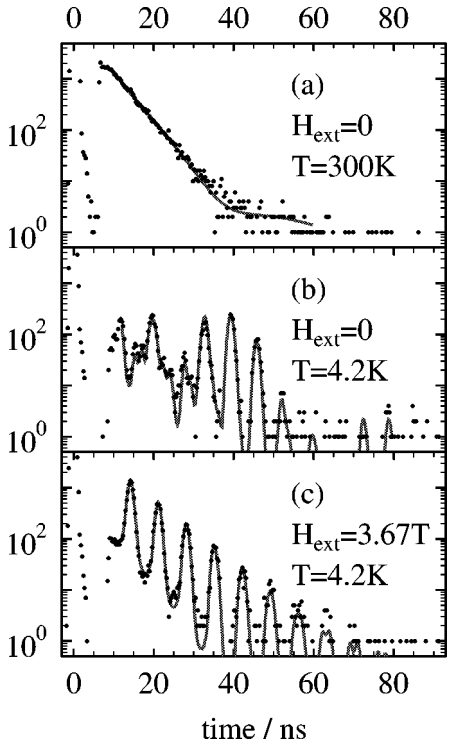

Figure 7. (a) Time spectrum of a EuS powder sample at room temperature. (b) Time spectrum of a EuS powder sample at $T = 4.2$ K. (c) Time spectrum of a EuS powder sample at $T = 4.2$ K in an externally applied field of 3.67 T parallel to the synchrotron radiation beam.

The dashed line shows the simulation of the time delayed intensity of an "ideal sandwich" with two samples of identical thickness, keeping all other parameters fixed.

The Eu(II)-chalcogenides are considered as model compounds for pure spin-magnetism. Within the EuX (X = O, S, Se, Te) series ferro- or antiferromagnetic ordering as well as pressure-induced structural phase transitions from the NaCl to the CsCl structure occur.

EuS, which is ferromagnetic below $T_C = 16.5$ K in the NaCl structure, was measured at room temperature (figure 7(a)) and at 4.2 K in zero field (figure 7(b)) as well as with an external magnetic field applied parallel to the synchrotron radiation beam (figure 7(c)). The fits clearly reveal an unsplit resonance line at room temperature (no magnetic ordering), at 4.2 K a ferromagnetic hyperfine field of 31.17(6) T with random orientation of magnetization (without external field) and – with external magnetic field – a complete orientation of the magnetic moments corresponding to an orientation of the hyperfine fields antiparallel to the external field. The effective hyperfine field is reduced to 29.0(2) T.

3. ^{181}Ta

^{181}Ta is an attractive target for experiments with synchrotron radiation. It has a low-energy (6.2 keV) nuclear E1 ($9/2 \rightarrow 7/2$) transition. The long lifetime of this level ($\tau_0 = 8.73$ μs [24]) and the complementary narrow energy width ($\Gamma_0 = 7.5 \cdot 10^{-11}$ eV) together with a very large nuclear magnetic moment ($\mu_e = +5.28(9)\mu_N$, where μ_N is the nuclear magneton) make this resonance a very sensitive probe of hyperfine interactions [25–28].

Another motivation for the use of synchrotron radiation are the technical difficulties in the preparation of radioactive sources for ^{181}Ta Mössbauer spectroscopy. The source lines are usually broadened by crystal imperfections or by interstitial impurities such as oxygen or hydrogen [29,30]. These difficulties are reflected in the fact that the narrowest experimental linewidth observed so far in ^{181}Ta Mössbauer spectroscopy is about $15\,\Gamma_0$ [30]. In addition, the resonant 6.2 keV γ-radiation suffers from a strong background of the $L_{\alpha,\beta}$ fluorescence X-radiation of Ta. The use of

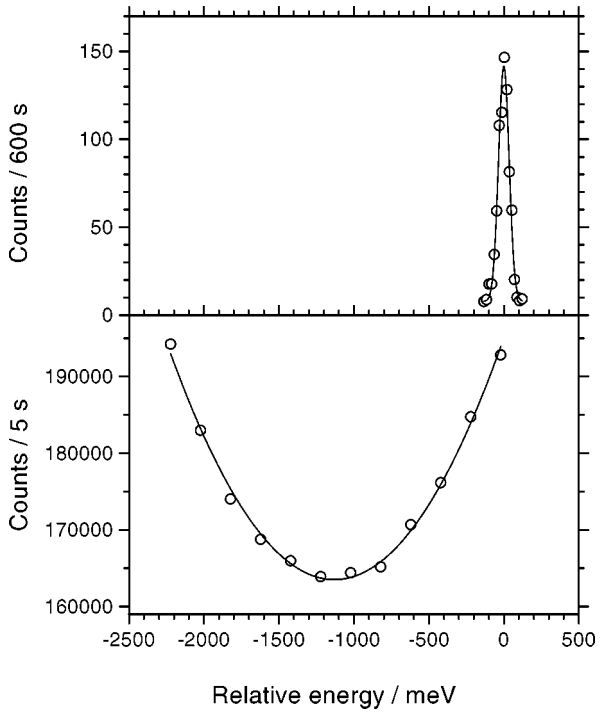

Figure 8. Determination of the ^{181}Ta resonance energy relative to the absorption fine structure of the Nd L_{III} edge: (a) delayed count rate of nuclear forward scattering of synchrotron radiation by a 7.5 μm Ta foil (in the time interval 40–90 ns after the prompt pulse). The solid line is a Gaussian fit to the experimental data with a FWHM of 83 ± 12 meV. (b) Intensity of radiation transmitted through the NdF_3 sample in the vicinity of the maximum absorption point. Experimental data in the displayed region are approximated by a parabola (solid line). Both sets of data are plotted as functions of energy relative to the ^{181}Ta resonance peak center. (From [6].)

synchrotron radiation promises to provide almost perfect experimental conditions. The short pulse of synchrotron radiation allows high-resolution time domain spectroscopy and the method is practically free of background radiation in a time window outside that of the synchrotron radiation pulses.

The first successful observation of nuclear scattering of X-rays by the ^{181}Ta resonance was reported in [6]. The experiment was performed at the 27-period wiggler beamline 6-2 at the Stanford Synchrotron Radiation Laboratory (SSRL). The resonant ^{181}Ta target was a 99.996% pure Ta foil of 15 mm diameter and 3.8 μm thickness. This sample had been previously studied by conventional Mössbauer spectroscopy [30] and revealed an extremely narrow experimental linewidth (measured as a convolution of the source and the absorber lines) of about 57 ± 1 μm/s ($15.8 \pm 0.3\,\Gamma_0$). For that experiment the sample was tilted at an angle of about 30°, so that its effective thickness along the beam path was about 7.5 μm.

The ^{181}Ta resonance was found at 6.214(2) keV. Note that the previously accepted value of the resonance energy 6.238(14) keV [31] was not precise enough. It turned out that ^{181}Ta is a rare lucky case, where the resonant energy almost exactly coincides with one of the known edges of an electron shell, namely, the Nd L_{III} edge. Figure 8 shows the position of nuclear resonance relative to the absorption maximum of Nd L_{III}. The resonance energy of ^{181}Ta is about 1 eV above the maximum absorption point. This feature greatly simplifies the search for the ^{181}Ta nuclear resonance in future experiments. In later studies at the ESRF [32,33], the resonance was found immediately.

The time distribution of nuclear forward scattering from the nonmagnetised Ta foil (measured at the SSRL) is shown in figure 9. The experimental data may be approximately described by an exponential with decay time of 530 ± 80 ns. The experimental data were fitted using the dynamical theory of resonant nuclear scattering [34]. For an E1 nuclear transition with some inhomogeneous broadening, the response function $R(E)$, the energy-dependent complex amplitude of the wave field transmitted through the absorber, has the form [35,36]:

$$R(E) = \exp \frac{-(\mathrm{i}T\Gamma_0/4)(1 + 2\mathrm{i}\xi)}{E - E_0 + \mathrm{i}\Gamma/2}; \tag{3.1}$$

where $T = \sigma_0 f_{\mathrm{LM}} n z = 44$ is the effective resonant thickness of the sample; $\sigma_0 = 1.1 \times 10^{-18}$ cm^2 the resonance cross-section; $f_{\mathrm{LM}} = 0.96$ the Lamb–Mössbauer factor; $n = 0.55 \times 10^{23}$ cm^{-3} the density of resonant nuclei; z the thickness of the sample; $(E - E_0)$ the deviation from the resonance energy; Γ the inhomogeneously broadened width of the resonance and $\xi = -0.16$ [37] a parameter which accounts for the interference between electronic scattering and nuclear scattering for the E1 transition of ^{181}Ta [35,36]. The best fit (solid line in figure 9) was obtained with a width of the nuclear resonance $\Gamma = 6 \pm 2\,\Gamma_0$, corresponding to 22 ± 7 μm/s. This broadening was later confirmed at the ESRF [32,33].

The ability to determine directly the width of the nuclear resonance in a sample is one of the advantages of synchrotron nuclear spectroscopy. In standard Mössbauer

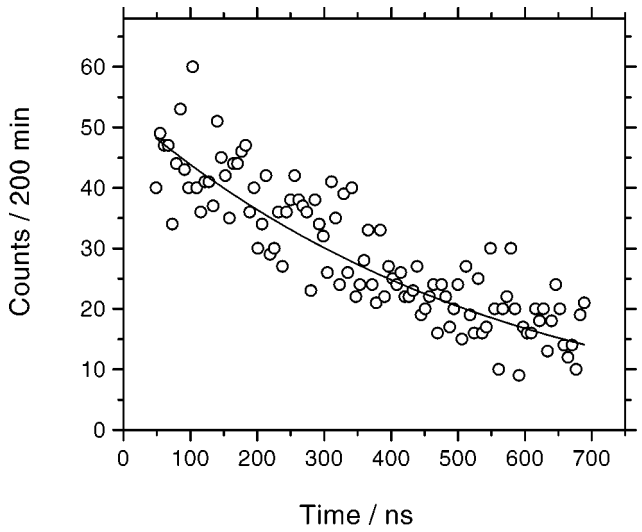

Figure 9. Time distribution of nuclear forward scattering of synchrotron radiation by the 7.5 μm Ta foil. The experimental data are fitted (solid line) by the dynamical theory of resonant nuclear scattering for a inhomogeneously broadening of the resonance line. A small background (2.7 counts per channel in the figure) is included in the fit. The width of the nuclear resonance is found to be $\Gamma = 6 \pm 2\,\Gamma_0$, corresponding to 22 ± 7 μm/s. (From [6].)

spectroscopy the measured linewidth always includes a convolution with the linewidth of the radioactive source. On the contrary, the value obtained here for the inhomogeneous broadening of the nuclear transition, $\Gamma = 6 \pm 2\,\Gamma_0$, is characteristic of the sample, determined only by the chemical environment of the ^{181}Ta nuclei.

The ^{181}Ta transition is a peculiar case, because it has a famous asymmetry of the resonant line [38], caused by interference between the nuclear internal conversion and photoelectric absorption processes [35,36,39]. This interference was included in eq. (3.1). Calculations of the forward scattering time distribution over a larger time range show that the dynamical beats [40] in the time distribution are affected by this interference. However, the experimentally available time range, much smaller than the expected time of the first dynamical beat minimum for this sample (at about 2.9 μs), did not allow this effect to be studied.

Nuclear forward scattering from a magnetised Ta foil was studied at the nuclear resonance beamline (ID18) [15]. The same sample was used, but it was not inclined; the X-ray beam passed it perpendicular to its surface. The foil was magnetised by a horizontal magnetic field of about 0.4 T perpendicular to the direction of the X-ray beam. For the E1 ^{181}Ta nuclear transition this means an excitation of $\Delta m = 0$ hyperfine nuclear transitions. The measured time spectrum of nuclear forward scattering is shown in figure 10. It consists of several distinct pulses, which are separated by long time intervals without any detectable count rate. This feature is caused by the high spin of both the excited and ground states. The $(9/2 \rightarrow 7/2)$ transition allows eight $\Delta m = 0$ hyperfine nuclear transitions. The conditions for coherent constructive

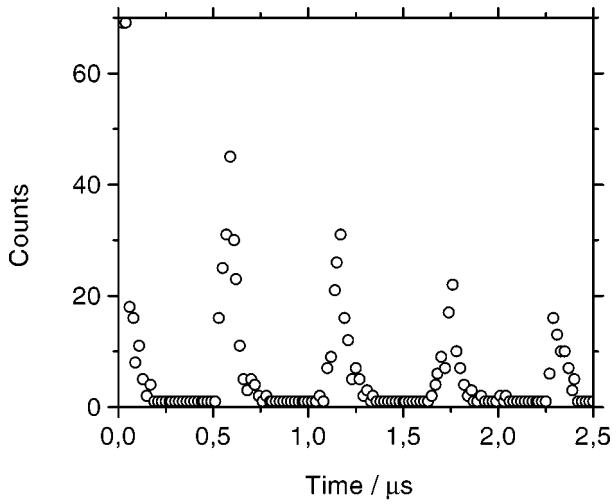

Figure 10. Time distribution of nuclear forward scattering of synchrotron radiation by a 3.8 μm thick Ta foil. The foil was magnetised by a horizontal magnetic field of about 0.4 T perpendicular to the direction of the X-ray beam. (From [32].)

scattering of X-rays by all sub-transitions are relatively rare (in this particular case once per about 600 ns). The intermediate peaks between the main maxima are greatly suppressed by an incomplete phasing of waves, scattered by various sublevels. One may directly show from eq. (3.1) that the quantum beat pattern is not influenced by the asymmetry parameter ξ. For instance, for the case of a thin absorber the asymmetry parameter determines just a common phase factor, which disappears when the intensity is calculated.

Further investigations of quantum beats in forward nuclear scattering by a ^{181}Ta foil were performed with both horizontal and vertical external magnetic field. Fits to the theory showed no sensitivity of the time spectra for the asymmetry parameter ξ. However, it revealed a very high sensitivity of data to the ratio of the magnetic moments of the excited and ground states [33].

The X-ray beam created by nuclear scattering in the Ta sample (the delayed, coherent forward scattered radiation), had a bandwidth of about 4.5×10^{-10} eV. This qualifies as the most monochromatic beam of synchrotron radiation ever prepared ($\Delta E/E = 7 \times 10^{-14}$). The longitudinal coherence length of such radiation is about 1 km.

4. ^{83}Kr

The 9.4 keV resonance of ^{83}Kr has a lifetime of 212 ns, which is convenient for synchrotron radiation studies. To date, there have been two published investigations, both largely demonstration experiments. The first, by Johnson et al. [4], demonstrated the possibility of doing nuclear forward scattering (NFS) from a monolayer coverage

of Kr (natural abundance 12%) on exfoliated graphite films. Independently, Baron et al. [5] measured incoherent nuclear scattering from gaseous krypton, demonstrating that it was possible to observe nuclear scattering of synchrotron radiation from a sample with zero Lamb–Mössbauer factor.

At present, little effort has been made to go beyond the two demonstration studies. There was one attempt to see beats in the incoherent channel using krypton gas [41], in a manner completely analogous to a perturbed angular correlation study. This was interesting because Kr gas should, in principle, be a simple system where the effects of forward scattering on the incoherent channel [42] could be neglected. However, this was hampered by low count rate (largely due to a poor filling mode of the storage ring). Likewise, some work[4] was done to extend the studies of Kr on exfoliated graphite to investigate the phase transition via measurement of the Lamb–Mössbauer factor (as in [43]).

In general, with the strong similarity between Kr and Fe resonances, there is little practical reason for not pursuing synchrotron radiation based studies. Some details make krypton slightly more difficult than iron, but not severely so. In particular, the slightly lower energy (9.4 instead of 14.4 keV) means that it is harder to make extremely high resolution monochromators. The highest order reflection available in silicon at room temperature is the (7 3 3) reflection, which has an intrinsic resolution of about 18 meV, so extreme asymmetries would be needed to achieve meV resolution. Another difference is the very low energy of the X-ray internal conversion products (M lines less than 2 keV), which means that, without great care, one would only detect nearly-elastic scattering events, which, effectively, might decrease counting rates in inelastic absorption measurements.

In conclusion, technically speaking, there are no strong impediments to Kr investigations using synchrotron radiation. What remains is to find a sufficiently strong scientific case. While nothing has presented itself as yet, one can speculate that continuation of the coverage studies mentioned above might be interesting; if one can obtain sufficient resolution, one could study the vibrational spectrum of Kr in cage (clathrate) compounds [44].

5. ^{169}Tm

The rare earth thulium occurs only as the isotope ^{169}Tm and has a low-energy nuclear resonance at 8.41 keV. The spin quantum numbers of ground state and excited state are $1/2$ and $3/2$, respectively. Nuclear level splittings caused by hyperfine interactions are therefore similar to those of ^{57}Fe and ^{119}Sn. The excitation of the 8.41 keV resonance of ^{169}Tm by synchrotron radiation has been demonstrated once in the past [1,45]. In the experiment, a pure nuclear reflection of a thulium iron garnet crystal was utilized to investigate hyperfine fields in the material. ^{169}Tm was the first non-iron isotope studied with synchrotron radiation. The selection was thought sensible

[4] This was work done at NSLS by D.E. Johnson et al. (the same group as in [4]).

under latter day circumstances, i.e., problems in proliferation of the new spectroscopy were anticipated by the need for isotopic enrichment and for optical components at 14.4 keV that were not well matched to the bending magnet synchrotron radiation sources. In fact, the isotope ^{169}Tm addressed both issues favorably, and the possibility to investigate single crystals with the highly collimated and polarized synchrotron radiation was attractive. However, the relatively large nuclear level width of 114 neV, equivalent to a lifetime of only 5.8 ns, turned out to be a major drawback. Whereas the development of optical components like monochromators [13] and polarization filters [20] has made phantastic progress in the past decade and new synchrotron radiation sources provided several orders of magnitude flux increase, the best reported time resolution of X-ray detectors improved only from about 1 ns [46] to 0.1 ns [47]. These developments did not favor use of the ^{169}Tm resonance, but other isotopes, particularly ^{57}Fe, were employed with great success.

Even with the present status of detector development, the short nuclear lifetime of ^{169}Tm is prohibitive for nuclear forward scattering, which is the preferred spectroscopic technique for the other nuclear isotopes. Although monochromators with meV resolution may be built, the strong prompt contribution to the time spectrum would make it very difficult to resolve the nuclear delayed signal. The most promising method might be to use a polarization filtering technique to suppress unwanted prompt contributions to the measured signal. The feasibility of this idea has been demonstrated for the ^{57}Fe isotope [20] and the obtained suppression of more than seven orders of magnitude can also be expected with similar optics [48] for samples containing ^{169}Tm. More recently, novel methods of measuring the vibrational density of states using incoherent nuclear resonant scattering are showing great potential [49,50]. However, the use of ^{169}Tm remains limited by the short lifetime and thus the inability to discriminate the nuclear delayed photons from the electronic scattering.

An interesting approach that uses the “nuclear lighthouse effect” was recently suggested [51] to permit time resolutions of better than 100 ps. The nuclear lighthouse effect encompasses the coherent reemission of delayed photons from a rotating resonant absorber. Depending on the time of reemission the resonantly scattered radiation is observed in a slightly changed direction. Since an angular change and rotation frequency are proportional, with sufficiently high rotation frequencies excellent “time resolutions” would result.

In conclusion, the application of nuclear resonant scattering techniques to the ^{169}Tm isotope depends crucially on detector improvements or the development of other means to obtain the required time resolution. With existing avalanche photodiode detectors one is limited to few cases, where a polarization filter can reduce the nonresonant, prompt scattering contributions.

6. ^{119}Sn

The ^{119}Sn isotope is a suitable nucleus for nuclear resonant scattering with synchrotron radiation because of its favorable resonance characteristics. The resonance

energy of 23.880 keV with 25.8 ns excited state lifetime, corresponding to an energy level width of 25.6 neV, is within reach of most high energy synchrotron radiation sources. The time separation between electron bunches ranges from a few ns to a few μs. A storage ring, operating in "timing" mode with a few hundred ns distance between the bunches is quite adequate for ^{119}Sn both for elastic or inelastic nuclear resonant scattering studies. The transition from $I_e = 3/2$ to $I_g = 1/2$ is converted via L-shell electrons with a conversion coefficient of $\alpha = 5.12$. The natural abundance of ^{119}Sn is 8.58%, and the nuclear resonant cross-section is $1.4 \cdot 10^{-18}$ cm^2.

The first observation of the ^{119}Sn resonance with synchrotron radiation was realized at the Cornell High Energy Synchrotron Source (CHESS), using a combination of a nested channel-cut crystal monochromator and a $^{119}SnO_2$/Pd-based grazing incidence antireflection film [2].

It was possible to measure the nuclear delayed signal with a plastic scintillation detector optically coupled to two photomultipliers and a time coincidence circuit. The crystal monochromator produced a 30 meV (FWHM) bandpass with an angular acceptance of 5.7 μrad [52]. This was accomplished by cutting the first Si(3 3 3) crystal asymmetrically. The Bragg angle for this energy is 14.38°, and the asymmetry angle was −11°. The 3.38° angle with an inch long first face allowed the use of a 1.3 mm height of the wiggler beam. The inner channel-cut crystal was a symmetric Si(5 5 5), and the combination had a total energy bandpass of 30 meV. The SnO_2/Pd GIAR film was specially designed to suppress electronic reflectivity at 2.09 mrad. The 43.2 nm SnO_2 was coated on 13 nm Pd. The zerodur substrate was 150 mm long, accepting a beam size of 0.3 mm, vertically. The electronic supression at 2.07 mrad was a factor of 45. At this angle, the energy bandpass of the GIAR film was 3.2 μeV. Due to the fast decay of ^{119}Sn nuclei with such a large bandpass, another sample of SnO was inserted in the beam to provide some time beats at later times so that an unambiguous determination of the delayed signal could be made. The experimental set-up is given in figure 11, the electronic reflectivity is given in figure 12, and the result of the measurement is in figure 13. The important aspect of this measurement was the

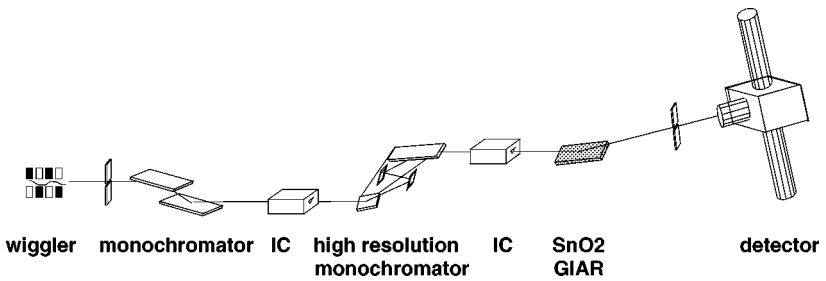

Figure 11. The set-up used in the first observation of the ^{119}Sn nuclear resonance at CHESS. The 24-pole wiggler, followed by a water cooled Si(1 1 1) monochromator produced a 3 eV bandpass X-ray beam incident on the high resolution monochromator, consisting of a Si(3 3 3)/Si(5 5 5) nested channel-cut pair. The $^{119}SnO_2$/Pd GIAR film is used as a nuclear monochromator and the reflected beam then transmitted through a SnO sample (not shown) to be detected by a time-resolved coincidence detector.

first use of high energy resolution optics above 20 keV, first use of a GIAR film as an optical component, and the fact that the ^{119}Sn nuclear resonance had been observed with synchrotron radiation.

The monochromators developed for ^{119}Sn have evolved quite fast. After the nested, 4-bounce channel-cut geometry based Si(3 3 3)/(5 5 5) monochromator with 30 meV bandpass, another monochromator, consisting of two Si(6 6 0) channel cuts placed dispersively against each other was described [3]. The energy bandpass of this arrangement was 50 meV, which was sufficient to observe nuclear forward scattering with an APD detector. Another nested channel-cut monochromator was described [53] in which a symmetric Si(12 12 12) crystal was inserted into an asymmetrically cut Si(6 4 2), resulting in an excellent energy resolution of 0.97 meV [53]. Flat crystal monochromators were first introduced for the ^{57}Fe resonance [54], resulting in a sub-meV bandpass, and then applied to ^{119}Sn [55]. These geometries are discussed in detail in [13], figure 5, and they are compared to monochromators for other isotopes in [13, table 1].

Advances in crystal monochromators with much higher energy resolution and detectors with better time resolution [56] have led to the first unambiguous observation of inelastic scattering from ^{119}Sn nuclei [53] and the first successful extraction of partial phonon density of states in SnO_2 [55]. In fact, it turns out that despite the shorter lifetime of ^{119}Sn compared to ^{57}Fe, the inelastic scattering measurements are just as easy, mainly because of the larger penetration and escape depth of 23.880 keV radiation.

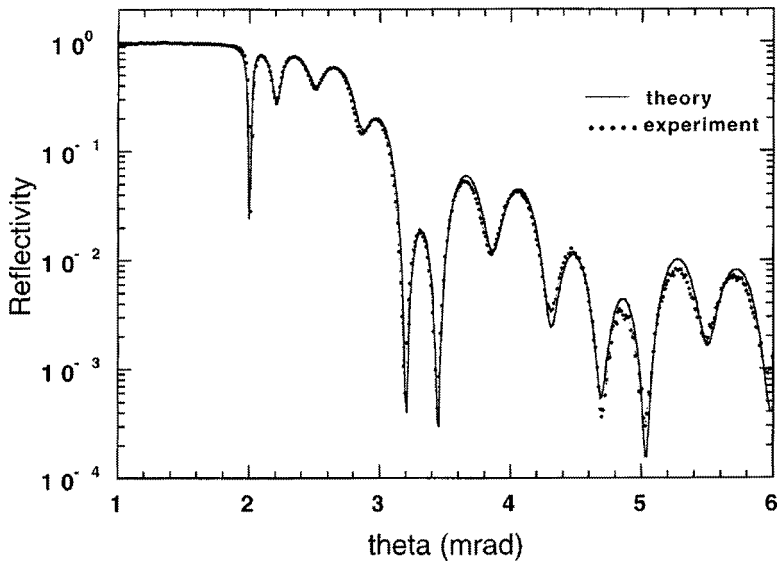

Figure 12. The electronic relectivity of the SnO_2/Pd GIAR film as a function of incidence angle, measured with "prompt" photons at 23.880 keV. The nuclear resonance experiment was carried out at 2.09 mrad in order to suppress nonresonant contributions to the signal detected by the plastic scintillator. The low angle position was chosen to maximize the nuclear reflectivity and energy bandpass.

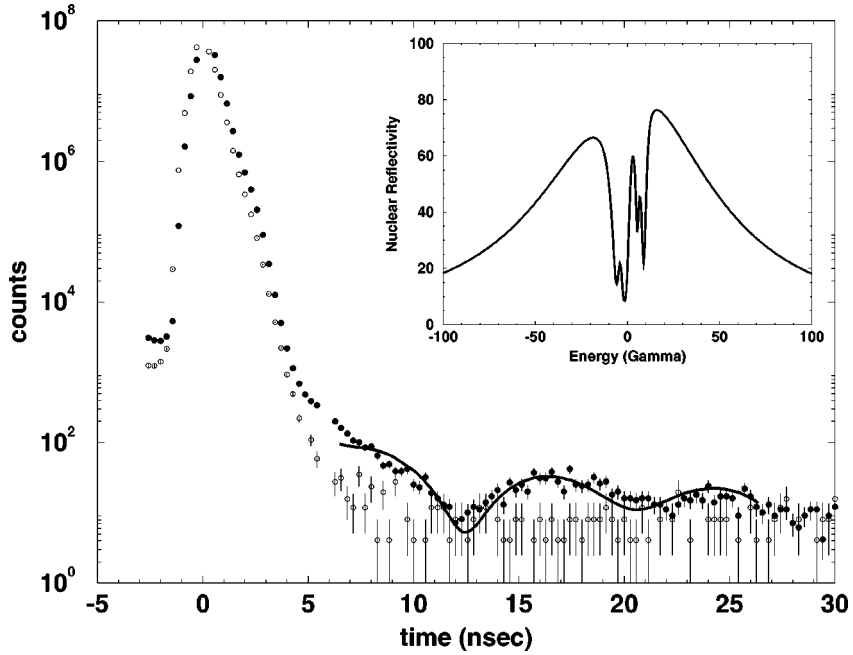

Figure 13. The time response of the ^{119}SnO sample, measured using a high energy resolution monochromator and a $^{119}SnO_2$/Pd GIAR film combination. The filled circles are the on-resonance spectrum, and the empty circles are off-resonance. The solid line is a theory simulation, superimposed onto the data. The inset shows the energy response of the combined SnO_2/Pd GIAR film and the SnO sample. The two doublets, separated by the isomer shift, cause the beat signal observed in the spectrum.

The incoherent scattering from Mössbauer nuclei can be observed through atomic fluorescence following nuclear absorption, by conversion electron emission, or by nuclear resonant fluorescence [50]. In the case of ^{119}Sn, the K-absorption edge is above the nuclear resonance energy, at 29.200 keV. The L-edge fluorescence lines between 3.4 and 4.1 keV have a low yield, about 7% (compared to 86% at the K-edge). Therefore, the observation of incoherent scattering is done by nuclear resonant fluorescence of 23.880 keV photons [53,55], despite the relatively low efficiency of the APD detectors, 6–12%, depending on the angle of incidence.

A measurement set-up for Sn inelastic nuclear resonant scattering using a 2-bounce high resolution monochromator is given in figure 14. The raw data for SnO, SnO_2 and $CaSnO_3$ are given in figure 15(a). In all these cases, it was possible to extract partial phonon density of states, which are given in figure 15(b).

The f-factors obtained from these data agree quite well with the literature. In addition, kinetic energy per atom and average force constants are obtained from the second and third moments of the spectra [57].

The ^{119}Sn isotope has another distinction among Mössbauer isotopes: it has been extensively used as a probe of lattice dynamics due to large variations in the recoilless fraction or f-factor. This value changes from a few percent in Sn metal to up to 66% in

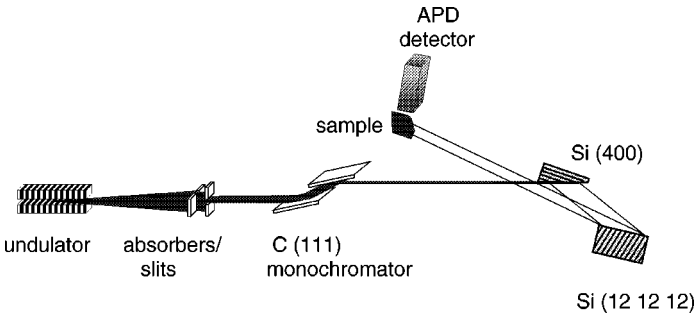

Figure 14. Schematic set-up of the experiments at the APS 3-ID beamline. The 88-pole undulator radiation is monochromatized to a bandpass of 2 eV by a water cooled double crystal diamond (1 1 1) monochromator. The bandpass of the high resolution monochromator is 3.6 meV. The APD detector is used to detect the 23.880 keV delayed nuclear fluorescence as a function of incident energy.

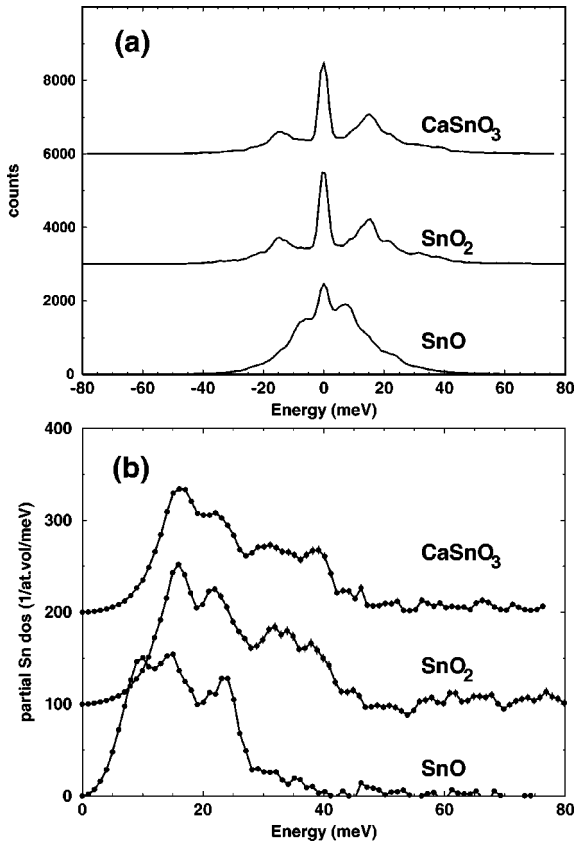

Figure 15. (a) Data obtained from inelastic nuclear resonant scattering from ^{119}Sn nuclei in various tin oxides with a 3.7 meV resolution monochromator. (b) The partial phonon density of states derived from the data. The similarity between SnO_2 and $CaSnO_3$, two different crystallographic structures with very similar arrangement of oxygen atoms around the Sn-atom, should be noted.

$CaSnO_3$. While the f-factor measurements from transmission Mössbauer spectroscopy suffer from large systematic errors, the extraction from the inelastic nuclear resonant scattering data is model independent. The determination of the partial phonon density of states is straightforward for f-factor values higher than 0.2, where the relative contribution of single phonon processes to the multiphonon processes can be reliably separated. Typically, the ratio of n-phonon events to $n-1$ phonon events is given by $-\ln f/n$. Unfortunately, for metallic β-Sn, the low f-factor prevented the extraction of phonon density of states from the raw data [53].

The isomer shift and quadrupole splitting in Sn compounds can also be measured using nuclear forward scattering. Since the bunch separation in modern storage rings corresponds to several lifetimes of ^{119}Sn, an accurate measurement should be possible. This aspect of the Sn-isotope has not been exploited, mainly because high resolution monochromators for ^{119}Sn are relatively new.

References

[1] W. Sturhahn, E. Gerdau, R. Hollatz, R. Rüffer, H.D. Rüter and W. Tolksdorf, Europhys. Lett. 14 (1991) 821.
[2] E.E. Alp, T.M. Mooney, T. Toellner, W. Sturhahn, E. Witthoff, R. Röhlsberger and E. Gerdau, Phys. Rev. Lett. 70 (1993) 3351.
[3] S. Kikuta, Hyp. Interact. 90 (1994) 335.
[4] D.E. Johnson, D.P. Siddons, J.Z. Larese and J.B. Hastings, Phys. Rev. B 51 (1995) 7909.
[5] A.Q.R. Baron, A.I. Chumakov, S.L. Ruby, J. Arthur, G.S. Brown, U. van Bürck and G.V. Smirnov, Phys. Rev. B 51 (1995) 16384.
[6] A.I. Chumakov, A.Q.R. Baron, J. Arthur, S.L. Ruby, G.S. Brown, G.V. Smirnov, U. van Bürck and G. Wortmann, Phys. Rev. Lett. 75 (1995) 549.
[7] O. Leupold, J. Pollmann, E. Gerdau, H.D. Rüter, G. Faigel, M. Tegze, G. Bortel, R. Rüffer, A.I. Chumakov and A.Q.R. Baron, Europhys. Lett. 35 (1996) 671.
[8] I. Koyama, Y. Yoda, X.W. Zhang, M. Ando and S. Kikuta, Japan. J. Appl. Phys. 35 (1996) 6297.
[9] C.M.P. Barton and N.N. Greenwood, in: *Mössbauer Effect Data Index*, eds. J.G. Stevens and V.E. Stevens (Plenum, New York, 1973) p. 395;
F. Grandjean and G.J. Long, in: *Mössbauer Spectroscopy Applied to Inorganic Chemistry*, Vol. 3, eds. G.J. Long and F. Grandjean (Plenum, New York, 1989) p. 513;
B. Harmatz, Nuclear Data Sheets 19 (1976) 33.
[10] B. Singh, J.A. Szücs and M.W. Johns, Nucl. Data Sheets 55 (1988) 185.
[11] R. Lübbers, G. Wortmann and H.F. Grünsteudel, this issue, section IV-2.3.
[12] O. Leupold and H. Winkler, this issue, section IV-2.5.
[13] T.S. Toellner, this issue, section VI-1.
[14] W.L. Bond, Acta Cryst. 13 (1960) 814.
[15] R. Rüffer and A.I. Chumakov, Hyp. Interact. 97/98 (1996) 589.
[16] T. Ishikawa, Y. Yoda, K. Izumi, C.K. Suzuki, X.W. Zhang, M. Ando and S. Kikuta, Rev. Sci. Instrum. 43 (1992) 824.
[17] A.Q.R. Baron, Nucl. Instrum. Methods A 352 (1995) 665.
[18] A.Q.R. Baron, this issue, section VI-2.
[19] W. Sturhahn and E. Gerdau, Phys. Rev. B 49 (1994) 9285.
[20] T.S. Toellner, E.E. Alp, W. Sturhahn, T.M. Mooney, X. Zhang, M. Ando, Y. Yoda and S. Kikuta, Appl. Phys. Lett. 67 (1995) 1993.
[21] E.E. Alp, W. Sturhahn and T. Toellner, Nucl. Instrum. Methods B 97 (1995) 526.

[22] O. Leupold, H. Grünsteudel, W. Meyer, H.F. Grünsteudel, H. Winkler, D. Mandon, H.D. Rüter, J. Metge, E. Realo, E. Gerdau, A.X. Trautwein and R. Weiss, in: *ICAME-95 Conf. Proc.*, Vol. 50, ed. I. Ortalli, SIF, Bologna (1996) p. 857.
[23] M. Pleines, Diplomarbeit, Universität Paderborn (1998).
[24] D. Mouchel, A. Nylandsted Larsen and H.H. Hansen, Z. Physik A 300 (1981) 85.
[25] G. Kaindl, D. Salomon and G. Wortmann, Phys. Rev. B 8 (1973) 1912.
[26] A. Heidemann, G. Kaindl, D. Salomon, H. Wipf and G. Wortmann, Phys. Rev. Lett. 36 (1976) 213.
[27] M.Löhnert, G. Kaindl, G. Wortmann and D. Salomon, Phys. Rev. Lett. 47 (1981) 194.
[28] V.K. Voitovetskii, S.M. Cheremisin and S.V. Sazonov, Phys. Lett. A 83 (1981) 81.
[29] C. Sauer, Z. Physik 222 (1969) 439.
[30] V.A. Dornow, J. Binder, A. Heidemann, G.M. Kalvius and G. Wortmann, Nucl. Instrum. Methods 163 (1979) 491.
[31] R.B. Firestone, Nucl. Data Sheets 62 (1991) 101.
[32] A.I. Chumakov et al., unpublished. (Measured in December 1995 at the Nuclear Resonance beamline (ID18) at the ESRF.)
[33] A.I. Chumakov, A.Q.R. Baron, L. Niesen, R. Rüffer et al., to be published. (Measured in June 1997 at the Nuclear Resonance beamline (ID18) at the ESRF.)
[34] Yu.M. Kagan, A.M. Afanasev and V.G. Kohn, J. Phys. C 12 (1979) 615.
[35] G.T. Trammell and J.P. Hannon, Phys. Rev. 180 (1969) 337.
[36] Yu.M. Kagan, A.M. Afanasev and V.K. Voitovetskii, Pisma Zh. Eksper. Teoret. Fiz. 9 (1969) 155 (JETP Lett. 9 (1969) 91).
[37] G. Kaindl and D. Salomon, Phys. Lett. B 32 (1970) 364.
[38] C. Sauer, E. Matthias and R.L. Mössbauer, Phys. Rev. Lett. 21 (1968) 961.
[39] H.C. Goldwire and J.P. Hannon, Phys. Rev. B 16 (1977) 1875.
[40] U. van Bürck, this issue, section IV-2.1.
[41] A.Q.R. Baron et al., attempt made at ESRF (1997).
[42] A.Q.R. Baron, A.I. Chumakov, R. Rüffer, H. Grünsteudel, H.F. Grünsteudel and O. Leupold, Europhys. Lett. 34 (1996) 331.
[43] U. Bergmann, S.D. Shastri, D.P. Siddons, B.W. Batterman and J.B. Hastings, Phys. Rev. B 50 (1994) 5957.
[44] Y. Hazoni, P. Hillman, M. Pasternak and S.L. Ruby, Phys. Lett. 2 (1962) 337.
[45] W. Sturhahn, Ph.D. dissertation, Universität Hamburg (1991).
[46] J. Metge, R. Rüffer and E. Gerdau, Nucl. Instrum. Methods A 292 (1990) 187.
[47] S. Kishimoto, J. Synchrotron Rad. 5 (1998) 275.
[48] T.S. Toellner, Ph.D. dissertation, Northwestern University (1996).
[49] A.I. Chumakov and W. Sturhahn, this issue, section V-1.1.
[50] W. Sturhahn and V.G. Kohn, this issue, section III-2.2.
[51] R. Röhlsberger, T.S. Toellner, W. Sturhahn, K.W. Quast, E.E. Alp, A. Bernhard, E. Burkel, O. Leupold and E. Gerdau, Phys. Rev. Lett. 84 (2000).
[52] T.M. Mooney, T.S. Toellner, W. Sturhahn, E.E. Alp and S.D. Shastri, Nucl. Instrum. Methods A 347 (1994) 348.
[53] A.I. Chumakov, A. Barla, R. Rüffer, J. Metge, H.F. Grünsteudel and H. Grünsteudel, Phys. Rev. B 58 (1998) 254.
[54] T.S. Toellner, M.Y. Hu, W. Sturhahn, K. Quast and E.E. Alp, Appl. Phys. Lett. 71 (1997) 2112.
[55] M. Hu, T.S. Toellner, W. Sturhahn, P.M. Hession, J.P. Sutter and E.E. Alp, Nucl. Instrum. Methods A 430 (1999) 430.
[56] S. Kishimoto, Rev. Sci. Instrum. 63 (1992) 824.
[57] W. Sturhahn and A.I. Chumakov, this issue, section V-1.2.